Predictive Data Transportation over Low-Altitude UAV Networks with Time-Varying Topology: A Dynamic Graph Approach

Bowen Li and Junting Chen
School of Science and Engineering (SSE) and Shenzhen Future Network of Intelligence Institute (FNii-Shenzhen)
The Chinese University of Hong Kong, Shenzhen, Guangdong 518172, China

***Abstract*—The rapidly growing human and autonomous robot activities in the low-altitude airspace brings new requirements and challenges to wireless networks. It is needed but challenging to design the aerial transmission strategy to ensure the transmission requirements of aerial nodes and avoid interference with ground terminals in a dynamic network topology. In this work, we study a predictive data transportation problem in aerial networks and formulate a integer programming problem to control the transmission route, handover time, and power. Specifically, a cache-and-pass transmission graph is introduced to convert the integer programming problem to a shortest path problem. Then, a graph-based alternating optimization algorithm with convergence guarantee is developed by using shortest path, alternating optimization algorithms. Simulation verifies that the proposed scheme is able to adjust the transmission strategy according to the data requirements in time-varying topology, reaching almost global optimality, and achieves an order of magnitude improvement compared with the classical static scheme, trivial routing scheme, and space-time routing scheme.**

***Index Terms*—Aerial communication networks, interference mitigation, route selection, predictive communication.**

I. Introduction

Unmanned aerial vehicle (UAV) communication networks are increasingly critical in diverse low-altitude UAV activities ranging from environmental monitoring to urban traffic management [1]. These networks enable UAVs to communicate with one another and ground stations, facilitating coordinated operations over vast areas. However, low-altitude aerial communications may generate substantial interference with ground wireless network due to the high probability of line-of-sight (LOS) conditions from the sky [2].

Power control and cache-and-pass transmission strategies are commonly employed to mitigate air-to-ground interference [3], [4]. The cache-and-pass strategy enables data transportation to occur at the optimal time, while the power control strategy ensures that transportation is conducted with the most efficient energy usage. Moreover, with the aid of radio maps [5], [6] and predetermined or inferred UAV trajectories, the future channel state information (CSI) can be predicted and used to guide the predictive communication design. However, aerial networks are highly dynamic with time-variant topologies due to UAV mobility, resulting in fluctuating link capacities and sometimes unavailable end-to-end paths. Therefore, how to select the transmission route and allocate transmission power and timing are challenging in the aerial communication networks.

Most existing works on aerial networks focused on independent UAV deployment, where generally, one dedicated UAV is deployed by trajectory optimization to perform various tasks [7], [8]. However, these UAVs operate independently and do not interact with each other, leading to poor performance when the source-to-destination distance is long. Some works sliced the dynamic aerial network in the time domain and coordinate UAVs using the instantaneous route from the sliced aerial network [9]. However, the end-to-end path is not always effective or efficient, especially in large networks. Some works optimized the handover time of nodes in the cache-and-pass transmission strategy to ensure the transmission occurs in good channel conditions [4]. However, they do not consider the route selection, which is still challenging in time-varying UAV topology, especially over a large timescale.

In a broader range of related literature, conventional communications in dynamic topology exploit graph theory to select transmission routes. Some works split the dynamic network into multiple static snapshots and select transmission paths in each snapshot graph [10]. To establish the temporal connections between the snapshots, some works proposed time-expanded graphs and developed time-space-combined routing algorithms [11], [12]. However, the transmission periods should not be uniform because of diverse link quality, and it is challenging to determine the duration of the snapshots. Some works utilized signal-to-noise ratio (SNR) or the relative positions to design snapshot duration [13]. However, they typically employ static thresholds for edge and duration establishment, neglecting the nuanced variations necessitated by specific data requirements. Moreover, such strategies commonly overlook the critical issue of interference, and it is still challenging to design the routing strategy for interference-aware communication requirements.

In this paper, we study the interference-aware communica-

The work was supported in part by the National Natural Science Foundation of China with grant No. 62171398, by the Basic Research Project No. HZQB-KCZYZ-2021067 of Hetao Shenzhen-HK S&T Cooperation Zone, by the Shenzhen Science and Technology Program under grant No. JCYJ20210324134612033, No. KQTD20200909114730003, and No. KJZD20230923115104009, by Guangdong Research Project with grant No. 2019QN01X895, and by Guangdong Basic and Applied Basic Research Foundation with grant 2024A1515011206.

tions in low-altitude aerial networks. Towards this end, two main technical challenges are needed to be addressed:

- How to select a route on time-varying topology.
- How to allocate transmission power and timing to adjust different data requirements.

To tackle these challenges, we develop a graph-based alternating optimization algorithm. It introduces a cache-and-pass transmission graph and converts the time-varying topology to a dynamic graph over the handover time. Then, an alternating optimization is performed to optimize the transmission route and transmission handover time. Our key contributions are made as follows:

- We propose a cache-and-pass transmission graph and convert the integer optimization problem to a shortest path problem for route optimization and a continuous problem for handover time optimization. Theoretically, it is proven that the shortest path problem in the proposed cache-and-pass transmission graph is identical to the optimization problem on the route, and the proposed graph-based alternating optimization algorithm is converged.
- We perform the numerical results to show that the proposed scheme is able to adjust the transmission strategy according to different data requirements in time-varying topology, reaching almost global optimality. Compared with the classical static, handover time optimization only, and space-time routing schemes, the proposed scheme can achieve an order of magnitude improvement.

II. System Model

Consider a group of N aerial nodes flying over an area, where a source node on the ground needs to transmit some data to a destination node at a distance. Assume that the trajectories of the aerial nodes are determined and fixed due to other missions of the aerial nodes. Consider exploiting the aerial nodes to relay the data from the source node to the destination node, as illustrated in Fig. 1. In addition, consider that there are M ground nodes that may be interfered by the transmission of the aerial nodes. The positions of source, destination, aerial nodes, and ground interference-sensitive nodes are known and denoted as $\boldsymbol{q}_n(t) \in \mathbb{R}^3$, where $n = 0$ represents the source node, $1 \leq n \leq N$ refers to the aerial nodes, $n = N+1$ represents the destination node, and $N+2 \leq n \leq N+M+1$ refers to the neighboring nodes.

A. Channel model and radio map model

We consider a flat fading channel model, in which the channel power gain between two nodes $m \neq n \in \{0, \cdots, N+M+1\}$ is given by

$$h_{m,n} = g_{m,n}\xi_{m,n} \tag{1}$$

where g and ξ represent the channel gain due to the large- and small-scale fading, respectively. The small-scale fading ξ is random and follows a Gamma distribution $\mathrm{G}(\kappa, 1/\kappa)$ with shape parameter κ, and the scale parameter is chosen as $1/\kappa$ to normalize the mean of ξ to 1.

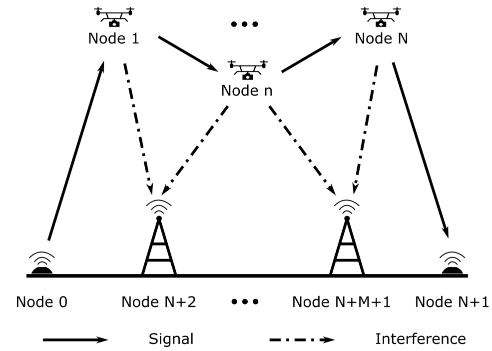

Figure 1. Aerial communication system illustration.

Assume that the system has access to the large-scale channel parameters, including the large-scale channel gain g and the Gamma distribution parameter κ, via a radio map $\boldsymbol{\Theta}(\boldsymbol{q}_m, \boldsymbol{q}_n) = (g_{m,n}, \kappa_{m,n})$ that records the large-scale channel parameters $g_{m,n}$ and $\kappa_{m,n}$ as a function of the transmitter and receiver locations $\boldsymbol{q}_m$ and $\boldsymbol{q}_n$ [5], [6].

With the aid of the radio map $\boldsymbol{\Theta}$ and the known locations of the aerial nodes at time t, $\boldsymbol{q}(t)$, the large-scale channel parameters at time t are $(g_{m,n}(t), \kappa_{m,n}(t)) = \boldsymbol{\Theta}(\boldsymbol{q}_m(t), \boldsymbol{q}_n(t))$. Thus, the power gain at time t, $h_{m,n}(t)$ defined in (1), follows Gamma distribution $\mathrm{G}(\kappa_{m,n}(t), g_{m,n}(t)/\kappa_{m,n}(t))$.

B. Communication model

This paper considers opportunistic transmission and power control to minimize the possible air-to-ground interference. The data is transported between two nodes when the channel to target node is strong and the channels to ground nodes are weak. As a result, a small transmission power suffices for the transmission, and low possible air-to-ground interference is generated. Specifically, consider a *cache-and-pass* data transportation strategy, where the data is relayed sequentially from one aerial node to another. To simplify the interference management among the aerial nodes, only one link is activated at a time, and therefore, there is no interference among the aerial nodes.

Denote the transmission route as $\boldsymbol{o} = \{o_n\}_{n\in\mathcal{N}}$, where $\mathcal{N} \triangleq \{0, 1, \cdots, N+1\}$, $o_n \in \mathcal{N}$ for all $n \in \mathcal{N}$ represents the index of the nth relay, and $o_0 = 0$, $o_{N+1} = N+1$ represent the source node and destination node.

Define the *handover time* variable $\boldsymbol{t} = \{t_n\}_{n\in\mathcal{N}}$ with $0 = t_0 \leq t_1 \leq \cdots \leq t_N \leq t_{N+1} = T$ for the data passing among nodes, where node o_n only transmits to node o_{n+1} in the nth transmission period $[t_n, t_{n+1})$.

Denote the transmission power of node o_n as $p_n > 0$, then the expected normalized capacity from node o_n to node o_{n+1} at time t can be computed as

$$\begin{aligned} c_n(t) &\triangleq \mathbb{E}\left\{\log\left(1 + p_n(t)\, h_n(t)\right)\right\} \\ &\geq \log\left(1 + p_n(t)\, g_n(t)\right) - \epsilon_n(t) \end{aligned}$$

where $\epsilon_n(t) \triangleq \log(e)/\kappa_n(t) - \log(1 + (2\kappa_n(t))^{-1})$ is the expected capacity loss due to uncertainty according to [14, Lemma 1], $h_n(t) \triangleq h_{o_n,o_{n+1}}(t)$, $g_n(t) \triangleq g_{o_n,o_{n+1}}(t)$, and $\kappa_n(t) \triangleq \kappa_{o_n,o_{n+1}}(t)$.

Meanwhile, the interference from node o_n under the transmission power p_n for the mth, $m \in \mathcal{M} \triangleq \{N+2, \cdots, N+M+1\}$, neighboring node at time slot t is modeled as

$$I_m(t) = \mathbb{E}\{h_{o_n,m}(t)\, p_n(t)\} = g_{o_n,m}(t)\, p_n(t).$$

This paper aims to optimize route of the data transportation among the aerial nodes $\boldsymbol{o}$, the handover time $\boldsymbol{t}$, and power control $\boldsymbol{P} = \{p_n(t)\}_{n\in\mathcal{N}, t\in[0,T]}$ for T time ahead for the transmission for minimizing the cost $F(\boldsymbol{P})$ and controling the instantaneous interference to the ground nodes, while delivering S bits of data from source to the destination

$$\mathscr{P}1: \underset{\boldsymbol{o},\boldsymbol{t},\boldsymbol{P}}{\text{minimize}} \quad F(\boldsymbol{P}) \tag{2}$$

$$\text{subject to} \quad \Upsilon_n(\boldsymbol{o},\boldsymbol{t},\boldsymbol{P}) = \int_{t\in\boldsymbol{t}_n} c_n(t)\, dt \geq S, \forall n \tag{3}$$

$$I_m(t) \leq I_{\text{th}}, \forall m, t \tag{4}$$

$$\boldsymbol{o} \in \Omega \tag{5}$$

$$\boldsymbol{t} \in \mathcal{T} \tag{6}$$

where Υ_n is the throughput from node o_n to node o_{n+1} during the interval $\boldsymbol{t}_n \triangleq [t_n, t_{n+1})$, I_{th} is the instantaneous interference threshold, $\Omega \triangleq \{\{o_n\}_{n\in\mathcal{N}} : o_n \in \mathcal{N}, \forall n; o_0 = 0; o_{N+1} = N+1\}$ represents the route space, and $\mathcal{T} \triangleq \{\{t_n\}_{n\in\mathcal{N}} : 0 = t_0 \leq t_1 \leq \cdots \leq t_K \leq t_{K+1} = T\}$ represents the handover time space. One possible choice of the objective (cost) function is the total transmission energy

$$F(\boldsymbol{P}) \triangleq \sum_{n\in\mathcal{N}} \int_{t\in\boldsymbol{t}_n} p_n(t)\, dt \tag{7}$$

to represent the possibility of air-ground interference.

C. Dynamic graph model

In order to optimize the transmission route, the time-varying aerial network is modeled as a dynamic graph with $N+1$ directed sub-graphs, as shown in Fig. 2. Specifically, the opportunistic transmissions in each period $\boldsymbol{t}_n$ is modeled as a directed sub-graph, where the vertices $\boldsymbol{V} = \{v_i\}_{i\in\mathcal{N}}$ are the communication nodes $n \in \mathcal{N}$, the edges $\boldsymbol{E} = \{e_{i,j}\}_{v_i,v_j\in\boldsymbol{V}}$ are the possible transmission links, and the weights $\boldsymbol{W} = \{w_{i,j}(\boldsymbol{t}_n)\}_{e_{i,j}\in\boldsymbol{E}, n\in\mathcal{N}}$ are the cost of transmission during each period $\boldsymbol{t}_n$. As a result, the weight of edge $e_{i,j}$ in t_n and t_{n+1}, which refers the transmission from node i to node j during the period $\boldsymbol{t}_n$, is given by the solution to the following problem

$$\mathscr{P}1\text{-}1: \quad \underset{\boldsymbol{p}_n}{\text{minimize}} \quad \int_{t\in\boldsymbol{t}_n} p_n(t)\, dt$$

$$\text{subject to} \quad \int_{t\in\boldsymbol{t}_n} c_n(t)\, dt \geq S,\ I_m(t) \leq I_{\text{th}}, \forall m, t$$

where $\boldsymbol{p}_n \triangleq \{p_n(t)\}_{t\in\boldsymbol{t}_n}$. Problem $\mathscr{P}1$-1 can be solved by a Lagrangian-based algorithm [14, Algorithm 1] with computational complexity $\mathcal{O}(t_{n+1} - t_n)$.

Note that the transmission handover times are not always uniform and the weight $w_{i,j}(\boldsymbol{t}_n)$ is varied over different $\boldsymbol{t}_n$. On the other side, the optimal handover time $\boldsymbol{t}$ depends on different transmission route. Therefore, the optimization problems on the handover time and the transmission route are connected by the dynamic graph model. However, how to determine the transmission route and how to optimize handover time are still challenging.

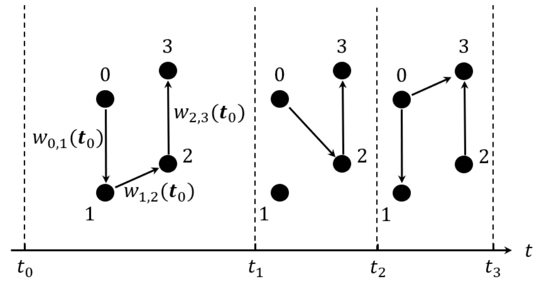

Figure 2. Dynamic graph illustration, where the sub-graph within two handover time represents one opportunistic transmission, and the graphs are changed when handover time is changed.

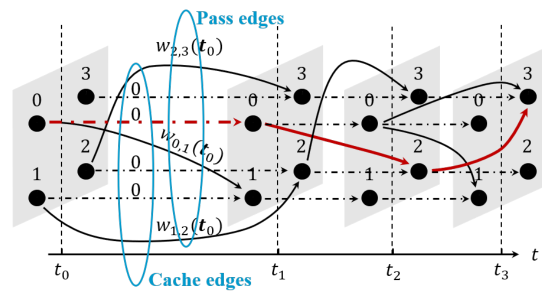

Figure 3. Cache-and-pass transmission graph illustration, where there are two types of edges, pass edges assigned with the dynamic transmission cost $w_{i,j}(\boldsymbol{t}_n)$, cache edges assigned with cost 0. The path with red edges is one example of transmitting from node 0 to node 3, where node 0 caches the data until t_1 when it starts to deliver the data to node 2. Then node 2 delivers the data to node 3.

III. Graph-based Alternating Optimization

We block the variables into two groups, $\{\boldsymbol{o}, \boldsymbol{P}\}$ and $\{\boldsymbol{t}, \boldsymbol{P}\}$, and optimize them alternatively. Firstly, we introduce a cache-and-pass transmission graph to convert the route optimization problem to a shortest path problem. Then we optimize handover time and power control by alternating and gradient optimization techniques.

A. Graph-based routing optimization

Given the handover time $\boldsymbol{t}$, the transmission strategy predictive problem $\mathscr{P}1$ is

$$\mathscr{P}1\text{-}2: \quad \underset{\boldsymbol{o},\boldsymbol{P}}{\text{minimize}} \quad (2) \quad \text{subject to} \quad (3)\text{-}(5).$$

In order to optimize the route, we introduce a cache-and-pass transmission graph, as shown in Fig. 3, where in each period $\boldsymbol{t}_n$, nodes can determine to cache or pass the data. If node i chooses to pass the data to node j during period $\boldsymbol{t}_n$, cost $w_{i,j,n} = w_{i,j}(\boldsymbol{t}_n)$ will consume, such that weight $w_{i,j}(\boldsymbol{t}_n)$ is assigned to the edge $e_{i,j,n}$; if node i chooses to cache the data during $\boldsymbol{t}_n$, no cost will consume, such that weight $w_{i,i,n} = 0$ is assigned to the edge $e_{i,i,n}$. Without loss of generality (w.l.o.g.), we set the sub-graphs for the vertex sets of adjacent layers be an unidirectional complete bipartite graph, and the weight is infinity if there is no possible for transmission.

In summary, the cache-and-pass transmission graph is $\mathscr{G}_s = (\{v_{i,n}\}_{i\in\mathcal{N},n\in\mathcal{N}}, \{e_{i,j,n}\}_{i\in\mathcal{N},j\in\mathcal{N},n\in\mathcal{N}}, \{w_{i,j,n}\}_{i\in\mathcal{N},j\in\mathcal{N},n\in\mathcal{N}})$. Since every vertex $v_{i,n}$, $i \in \mathcal{N}$, in layer n only directional connects the vertex $v_{j,n+1}$, $j \in \mathcal{N}$, in the next layer, *i.e.*, layer $n+1$, for clarification, we denote the path in graph $\mathscr{G}_s$ as $\boldsymbol{r} = \{v_{\mu_n,n}\}_{n\in\mathcal{N}}$.

Remark 1. Mapping from graph $\mathscr{G}_s$ to optimization problem $\mathscr{P}$1-2

(i) A path $\boldsymbol{r} = \{v_{\mu_n,n}\}_{n\in\mathcal{N}}$ from vertex $v_{0,0}$ to vertex $v_{N+1,N+1}$ in graph $\mathscr{G}_s$ represents the transmission route $\boldsymbol{o} = \{o_n = \mu_n\}_{n\in\mathcal{N}}$.

(ii) The distance of the path $\boldsymbol{r}$, denoted as $d(\boldsymbol{r})$, is identical to the optimal solution to problem $\mathscr{P}$1 when given handover time $\boldsymbol{t}$ and transmission order $\boldsymbol{o}$, *i.e.*, $F(\boldsymbol{P}^*(\boldsymbol{o},\boldsymbol{t}))$.

(iii) Denote the space of the path from vertex $v_{0,0}$ to vertex $v_{N+1,N+1}$ in graph $\mathscr{G}_s$ as $\mathcal{R}$. The transmission route set $\{\boldsymbol{o}\}$ obtained from $\boldsymbol{r} \in \mathcal{R}$ is identical to the transmission route space Ω.

It is proven that the route and power control along the shortest path from vertex $v_{0,0}$ to vertex $v_{N+1,N+1}$ in graph $\mathscr{G}_s$ is the optimal solution to problem $\mathscr{P}$1-2.

Proposition 2. *(Necessary and sufficient condition of optimality.) Given the the shortest path $\boldsymbol{r} = \{v_{\mu_n,n}\}_{n\in\mathcal{N}}$ from vertex $v_{0,0}$ to vertex $v_{N+1,N+1}$ in graph $\mathscr{G}_s$, the route $\boldsymbol{o} = \{\mu_n\}_{n\in\mathcal{N}}$ and power control $\boldsymbol{p}_n = \boldsymbol{p}_n^*(o_n = \mu_n, o_{n+1} = \mu_{n+1}; \boldsymbol{t})$ is identical to the optimal solution to problem $\mathscr{P}$1-1, where $\boldsymbol{p}_n^*(o_n, o_{n+1}; \boldsymbol{t})$ is the optimal solution to problem $\mathscr{P}$1-2.*

Proof: If the path $\boldsymbol{r}$ is the shortest path from vertex $v_{0,0}$ to vertex $v_{N+1,N+1}$ in graph $\mathscr{G}_s$, that is, for any other path $\boldsymbol{r}' \in \mathcal{R}\backslash\{\boldsymbol{r}\}$, the distance of $\boldsymbol{r}'$ is less or equal to the distance of $\boldsymbol{r}$. In other word, $F(\boldsymbol{P}^*(\boldsymbol{o},\boldsymbol{t})) \leq F(\boldsymbol{P}^*(\boldsymbol{o}',\boldsymbol{t})), \forall \boldsymbol{o}' \in \Omega\backslash\boldsymbol{o}$ according to Remark 1, where $\boldsymbol{o}$ and $\boldsymbol{o}'$ are the transmission order obtained by $\boldsymbol{r}$ and $\boldsymbol{r}'$. As a result, the transmission order $\boldsymbol{o}$ along with the transmission policy $\boldsymbol{p}_n = \boldsymbol{p}_n^*(o_n = \mu_n, o_{n+1} = \mu_{n+1}; \boldsymbol{t}), \forall n \in \mathcal{N}$ is the optimal solution to problem $\mathscr{P}$1-1. Vice versa. ■

As a result, the routing optimization problem becomes a shortest path problem in a static graph, which can be solved by mature algorithm.

B. Handover time optimization

Given the transmission route $\boldsymbol{o}$,[1] the transmission strategy predictive problem $\mathscr{P}$1 becomes

$$\mathscr{P}1\text{-}3: \quad \underset{\boldsymbol{t},\boldsymbol{P}}{\text{minimize}} \quad (2) \quad \text{subject to} \quad (6).$$

[1]W.l.o.g., we assume that there is no duplicate node in $\boldsymbol{o}$. If there is, we can merge the duplicate nodes without changing their orders and obtain a no-duplicate-node sequence, as shown in Fig. 4.

Algorithm 1 Graph-based alternating optimization algorithm.

\# Initialization: $\boldsymbol{t}^{(0)} \leftarrow [0, T/(N+1), \cdots, T]$, $\kappa = 0$.

1) Construct the cache-and-pass transmission graph $\mathscr{G}_s$, and develop the optimal route $\boldsymbol{o}$ by finding the shortest path in graph $\mathcal{G}_s$ as shown in Proposition 2;
2) Merge the duplicate nodes in $\boldsymbol{o}$ to $\boldsymbol{o}'$ and update the transmission handover time $\boldsymbol{t}$ to $\boldsymbol{t}'$;
3) Alternatively optimize handover time $\boldsymbol{t}'$ by backtracking gradient descent method and optimize power control $\boldsymbol{P}'$ by Lagrangian-based algorithm, until $\nabla_{\boldsymbol{t}'} \to 0$;
4) Duplicate the merged node in $\boldsymbol{o}'$ to $\boldsymbol{o}$, and update the handover time $\boldsymbol{t}'$ to $\boldsymbol{t}$ based on $\boldsymbol{P}'$.
5) Update $\kappa \leftarrow \kappa + 1$, $\boldsymbol{t}^{(\kappa)} \leftarrow \boldsymbol{t}$, $\boldsymbol{o}^{(\kappa)} \leftarrow \boldsymbol{o}$, $\boldsymbol{P}^{(\kappa)} \leftarrow \boldsymbol{P}$; Then go to step 1 until $\boldsymbol{t}^{(\kappa)} = \boldsymbol{t}^{(\kappa-1)}$ and $\boldsymbol{o}^{(\kappa)} = \boldsymbol{o}^{(\kappa-1)}$.

\# Output $\boldsymbol{t}^{(\kappa)}$, $\boldsymbol{o}^{(\kappa)}$, and $\boldsymbol{\phi}^{(\kappa)}$.

We solve problem $\mathscr{P}$1-3 by alternative optimization technique. Firstly, given handover time $\boldsymbol{t}$, the power control optimization problem becomes several independent power lalocation problems, as problem $\mathscr{P}$1-1, and can be solved by a Lagrangian-based algorithm [14, Algorithm 1]. Then using the updated qth round of power control $\boldsymbol{p}^{(q)}$, the handover time can be updated by backtracking gradient method $\boldsymbol{t}^{(q)} = \boldsymbol{t}^{(q-1)} - \alpha^{(q)} \frac{\nabla_{\boldsymbol{t}}}{||\nabla_{\boldsymbol{t}}||}$, where $\alpha^{(q)}$ is the backtracking step size, $\nabla_{\boldsymbol{t}} \triangleq [\nabla_{t_1}, \nabla_{t_2}, \cdots, \nabla_{t_N}]^T$ is the partial derivative of the objective function over the handover time t_n, and

$$\begin{aligned}\nabla_{t_n} =& \frac{\partial}{\partial t_n}\left(\int_{t_{n-1}^{(q-1)}}^{t_n} p_{n-1}^{(q)}(t)\,dt + \int_{t_n}^{t_{n+1}^{(q-1)}} p_n^{(q)}(t)\,dt\right)\\ =& p_{n-1}^{(q)}(t_n) - p_n^{(q)}(t_n).\end{aligned}$$

C. Graph-based alternating optimization algorithm

Based on the graph-based routing optimization approach and the handover time optimization approach, we propose a graph-based alternating optimization algorithm, as shown in Algorithm 1. Specifically, we first construct a cache-and-pass transmission graph $\mathscr{G}_s$ and update the route $\boldsymbol{o}$ and power control $\boldsymbol{P}$ by finding the shortest path in graph $\mathcal{G}_s$, as shown in Proposition 2. Then, we merge the duplicate nodes in $\boldsymbol{o}$ to $\boldsymbol{o}'$ and update the transmission handover time $\boldsymbol{t}$ to $\boldsymbol{t}'$ accordingly, for satisfying the handover time optimization condition. Correspondingly, we duplicate the merged node in $\boldsymbol{o}'$ to $\boldsymbol{o}$ after finishing handover time optimization to make sure no change on the structure of graph $\mathscr{G}_s$.

Fig. 4 illustrates a round of alternating optimization process. By merging the duplicate nodes from step 1) to step 2), the periods of each transmission are non-decreasing. For example, the transmission from node 1 to node 2 occurs on $[1, 2)$, while it becomes $[0, 2)$ after duplicate nodes merging. On the other side, duplicating the merged nodes does not change the actual optimal transmission period. For example, while the allowed transmission period is $[0, 2.5)$ for the transmission from node 1 to node 2 before duplicating, the actual optimal transmission period is $[0.5, 2.5)$. Thus, shrinking the allowed transmission

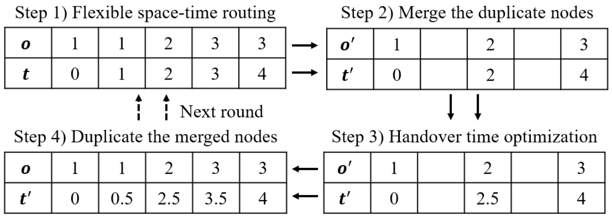

Figure 4. Illustration of a single iteration in the graph-based alternating optimization process, where the transmissions occurs during $[0.5, 2.5)$ for node 1 to node 2, and during $[2, 5, 3.5)$ for node 2 to node 3 after handover time optimization in step 3).

period from $[0, 2.5)$ to $[0.5, 2.5)$ does not affect the actual optimal transmission period.

According to the non-decreasing transmission period properties during the merge and duplicate process, it is proven, in the following proposition, that the proposed graph-based alternating optimization algorithm is converged.

Proposition 3. *(Convergence.) The algorithm 1 is converged.*

Proof: Denote the cost after step ι in round κ as $F_\iota^{(\kappa)}$, we will prove that the $F_1^{(\kappa)} \geq F_2^{(\kappa)} \geq F_3^{(\kappa)} = F_4^{(\kappa)} \geq F_1^{(\kappa+1)}$, ensuring that the cost over rounds is non-increasing, thereby demonstrating algorithm convergence over iterations.

Firstly, $F_1^{(\kappa)} \geq F_2^{(\kappa)}$ because the non-decreasing transmission periods over the duplicate node merging process decrease the cost of each transmission. $F_2^{(\kappa)} \geq F_3^{(\kappa)}$ because the backtracking gradient descent method guarantees optimizing towards low cost. $F_3^{(\kappa)} = F_4^{(\kappa)}$ because the actual optimal transmission periods of each transmission are unchanged before and after duplicating. $F_4^{(\kappa)} \geq F_1^{(\kappa+1)}$ because the route can be converted to a path in graph $\mathscr{G}_s$ and the shortest distance $F_1^{(\kappa+1)}$ must be less than $F_4^{(\kappa)}$, that is the distance of one path in $\mathscr{G}_s$. ■

IV. Simulation

Consider a 400 m $\times$ 500 m area where 4 straight-line UAVs and one clockwise-circuit UAV run on predetermined trajectories, as shown in Fig. 5. The aerial nodes may suspend the communication service at the end points with a random duration following a uniform distribution $\mathcal{U}(0, D)$. One base station (BS) located in the center of the area performs as the ground node. The source and destination are random located in source and destination area, respectively. The data generated from the source node will be relayed to the destination node via the aerial nodes..

In this section, numerical results are provided to validate the proposed design. The source, two vertical UAVs, two horizontal UAVs, the destination, and one BS altitudes are fixed at 0 m, 45 m, 50 m, 0 m, and 5 m. The aerial node velocity is set randomly at 5-15 m/s to simulate transporting data from a sensor to a fusion center. The channel gains are realized by $h_{m,n} = g_{m,n}\xi_{m,n}$ according to (1), as [14]. The shape parameter $\kappa_{m,n}$ of Gamma distribution small-scale fading $\xi_{m,n}$ is chosen randomly from 1 to 30, large-scale fading $g_{m,n}$

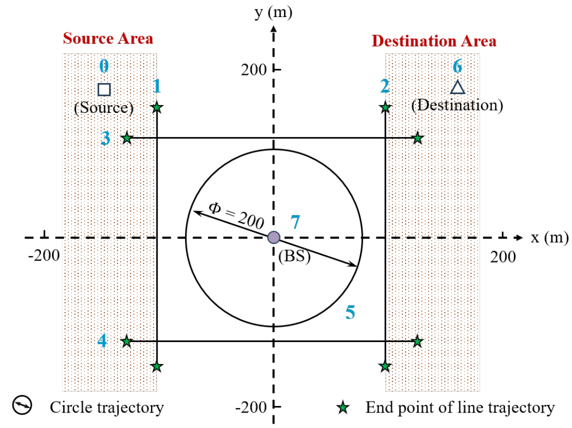

Figure 5. Illustration for aerial ad hoc networks for data delivering. The nodes with index from 0 to 7 represent the source, two vertical UAVs, two horizontal UAVs, the destination, and one BS, respectively.

Table I
PERFORMANCE WITH DIFFERENT TOLERABLE TIME T.

T (s)	$\boldsymbol{o}'$	$\boldsymbol{t}'$(s)	F	$F_{\text{0-3-6}}$
1	0-1-3-6	$[0, 0.153, 0.849, 1]$	5.113	1027
20	0-1-5-2-6	$[0, 3.333, 10.265, 13.33, 20]$	2.381	104.5
40	0-1-5-6	$[0, 6.667, 20, 40]$	0.193	78.60
60	0-3-6	$[0, 40, 60]$	0.022	0.026

is path loss, the propagation for LOS and non-line-of-sight (NLOS) links is taken from the 3GPP Urban Micro (UMi) model, and the blockage status between UAV and ground nodes is simulated by LOS probability model.

Table I to II list the route, handover time, and cost defined in (7), obtaining by the proposed predictive transmission strategy, under different tolerable time T, generating time t_0, respectively. In comparison, the cost $F_{\text{0-3-6}}$ of static route strategy, where the most frequent route 0-3-6 and the uniform transmission periods are performed. It is shown that the transmission strategy varies on the data requirement, and the proposed scheme can adjust the transmission strategy according to different data requirements. When the transmission is sensitive to the delay, through the nearest aerial nodes (node 1 for the source and node 3 for the destination when $T = 1$ s) as the relay is chosen, while in the non-sensitive case, the route with less relay is used, *e.g.*, when $T = 60$ s, thereby decreasing the cost. Compared with the traditional static route scheme, the proposed strategy generates significantly less cost. Similar results are shown in the different generating times in Table II.

Then, we compare the cost with the following baseline schemes, where the (initial) positions of nodes and data re-

Table II
PERFORMANCE WITH DIFFERENT GENERATING TIME t_0.

t_0(s)	$\boldsymbol{o}'$	$\boldsymbol{t}'$(s)	F	$F_{\text{0-3-6}}$
0	0-1-5-2-6	$[0, 3.333, 10.265, 13.33, 20]$	2.381	104.5
10	0-3-6	$[10, 15.479, 30]$	0.755	79.22
20	0-1-5-2-6	$[20, 30, 40]$	0.222	110.0
50	0-1-5-3-6	$[50, 53.33, 60, 69.79, 70]$	1.233	273.5

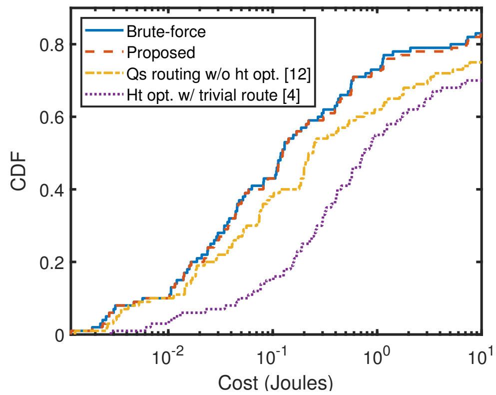

Figure 6. The CDF of the cost of 100 replicate experiments.

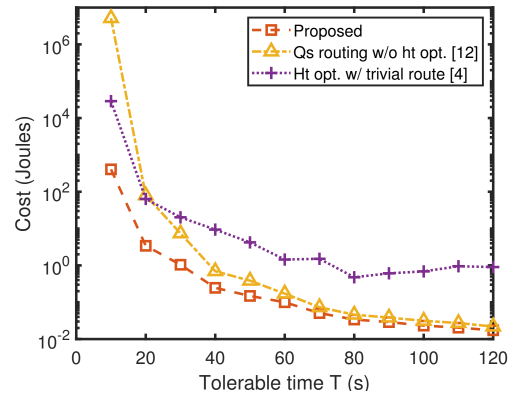

Figure 7. The average cost over different tolerable time.

quirements are random set.

1) Handover time optimization with trivial route selection (Ht opt w/ trivial route) [4]: This scheme chooses the nodes whose trajectories cross the source-destination line segment as the relays, and then perform handover time optimization.

2) Space-time routing (Qs routing w/o ht opt) [13]: This scheme optimizes the transmission route by the space-time routing algorithm but not optimize handover time.

3) Exhaustive searching (Brute-force): This scheme enumerates all possible paths from source to destination using the handover time optimization, and selects the path with least cost as the transmission route.

Fig. 6 shows the cumulative distribution function (CDF) of the cost of different schemes. It depicts that the performance of the proposed scheme is almost identical to the solution from exhaustive searching, which verifies the robust of the proposed algorithm. In addition, the proposed scheme outperforms the scheme with only route optimization about 1 times in median, and outperforms the scheme with only handover time optimization about 5 times in median.

Fig. 7 shows the average cost over different tolerable time T. It is shown that when the transmission is sensitive to the delay, the handover time optimization dominates the performance, while when the transmission is tolerable to the delay, the route selection dominates the performance. Furthermore, the proposed scheme, which accounts for both handover time and route, achieves performance enhancements exceeding an order of magnitude regardless of whether the transmission requirements are delay-sensitive or delay-tolerant.

V. Conclusion

This work developed a graph-based alternating optimization algorithm to control the aerial interference to ground nodes. Firstly, a cache-and-pass transmission graph is introduced and the route optimization problem is converted to a shortest path problem. Then, an alternating optimization problem is proposed to optimize handover time, route selection, as well as power control, with convergence guaranteed. Simulations verify that the proposed scheme is able to adjust the transmission strategy according to data requirements in time-varying topology, reaching almost global optimality, and achieve an order of magnitude improvement compared with classical schemes.

References

[1] G. Geraci, A. Garcia-Rodriguez, M. M. Azari, A. Lozano, M. Mezzavilla, S. Chatzinotas, Y. Chen, S. Rangan, and M. Di Renzo, "What will the future of UAV cellular communications be? a flight from 5G to 6G," *IEEE Commun. Surveys Tuts.*, vol. 24, no. 3, pp. 1304–1335, 2022.

[2] A. Rahmati, S. Hosseinalipour, Y. Yapici, X. He, I. Guvenc, H. Dai, and A. Bhuyan, "Dynamic interference management for UAV-assisted wireless networks," *IEEE Trans. on Wireless Commun.*, vol. 21, no. 4, pp. 2637–2653, 2022.

[3] C. Shen, T.-H. Chang, J. Gong, Y. Zeng, and R. Zhang, "Multi-UAV interference coordination via joint trajectory and power control," *IEEE Trans. Signal Process.*, vol. 68, pp. 843–858, 2020.

[4] B. Li and J. Chen, "Large timescale optimization for communications over aerial ad hoc networks with predetermined trajectories," *IEEE Trans. on Commun.*, 2024.

[5] Y. Zeng, J. Chen, J. Xu, D. Wu, X. Xu, S. Jin, X. Gao, D. Gesbert, S. Cui, and R. Zhang, "A tutorial on environment-aware communications via channel knowledge map for 6G," *IEEE Commun. Surveys Tuts.*, pp. 1–1, 2024.

[6] H. Sun and J. Chen, "Propagation map reconstruction via interpolation assisted matrix completion," *IEEE Trans. Signal Process.*, vol. 70, pp. 6154–6169, 2022.

[7] J. Zhang, Y. Zeng, and R. Zhang, "UAV-enabled radio access network: Multi-mode communication and trajectory design," *IEEE Trans. Signal Process.*, vol. 66, no. 20, pp. 5269–5284, 2018.

[8] K. Liu and J. Zheng, "UAV trajectory planning with interference awareness in UAV-enabled time-constrained data collection systems," *IEEE Trans. Veh. Technol.*, vol. 73, no. 2, pp. 2799–2815, 2024.

[9] S. Gangopadhyay and V. K. Jain, "A position-based modified OLSR routing protocol for flying ad hoc networks," *IEEE Trans. Veh. Technol.*, vol. 72, no. 9, pp. 12 087–12 098, 2023.

[10] J. Li, H. Lu, K. Xue, and Y. Zhang, "Temporal netgrid model-based dynamic routing in large-scale small satellite networks," *IEEE Trans. Veh. Technol.*, vol. 68, no. 6, pp. 6009–6021, 2019.

[11] J. A. Fraire, O. De JonckÃšre, and S. C. Burleigh, "Routing in the space internet: A contact graph routing tutorial," *J. Netw. Comput. Appl.*, vol. 174, p. 102884, 2021.

[12] F. Li, S. Chen, M. Huang, Z. Yin, C. Zhang, and Y. Wang, "Reliable topology design in time-evolving delay-tolerant networks with unreliable links," *IEEE Trans. Mobile Comput.*, vol. 14, no. 6, pp. 1301–1314, 2015.

[13] Z. Han, C. Xu, G. Zhao, S. Wang, K. Cheng, and S. Yu, "Time-varying topology model for dynamic routing in LEO satellite constellation networks," *IEEE Trans. Veh. Technol.*, vol. 72, no. 3, pp. 3440–3454, 2023.

[14] B. Li and J. Chen, "Radio map assisted approach for interference-aware predictive UAV communications," *IEEE Trans. on Wireless Commun.*, 2024.